JOURNAL OF GEOPHYSICAL RESEARCH, VOL. 112, D03209, doi:10.1029/2006JD007440, 2007

Cirrus clouds, humidity, and dehydration in the tropical tropopause layer observed at Paramaribo, Suriname (5.8°N, 55.2°W)

Franz Immler,[1] Kirstin Krüger,[2,3] Susann Tegtmeier,[2,4] Masatomo Fujiwara,[5] Paul Fortuin,[6] Gé Verver,[6] and Otto Schrems[1]

Received 25 April 2006; revised 21 September 2006; accepted 4 October 2006; published 10 February 2007.

[1] In the framework of the European Project STAR the Mobile Aerosol Raman Lidar (MARL) of the Alfred Wegener Institute (AWI) was operated in Paramaribo, Suriname (5.8°N, 55.2°W), and carried out extensive observations of tropical cirrus clouds during the local dry season from 28 September 2004 to 16 November 2004. The coverage with ice clouds was very high with 81% in the upper troposphere (above 12 km). The frequency of occurrence of subvisual clouds was found to be clearly enhanced compared to similar observations performed with the same instrument at a station in the midlatitudes. The extinction-to-backscatter ratio of thin tropical cirrus is with 26 ± 7 sr significantly higher than that of midlatitude cirrus (16 ± 9 sr). Subvisual cirrus clouds often occur in the tropical tropopause layer (TTL) above an upper tropospheric inversion. Our observations show that the ice-forming ability of the TTL is very high. The transport of air in this layer was investigated by means of a newly developed trajectory model. We found that the occurrence of clouds is highly correlated with the temperature and humidity history of the corresponding air parcel. Air that experienced a temperature minimum before the measurement took place was generally cloud free, while air that was at its temperature minimum during the observation and thus was saturated contained ice. We also detected extremely thin cloud layers slightly above the temperature minimum in subsaturated air. The solid particles of such clouds are likely to consist of nitric acid trihydrate (NAT) rather than ice.

Citation: Immler, F., K. Krüger, S. Tegtmeier, M. Fujiwara, P. Fortuin, G. Verver, and O. Schrems (2007), Cirrus clouds, humidity, and dehydration in the tropical tropopause layer observed at Paramaribo, Suriname (5.8°N, 55.2°W), *J. Geophys. Res.*, *112*, D03209, doi:10.1029/2006JD007440.

1. Introduction

[2] In the tropical tropopause region, ice clouds occur with high frequencies of up to 70% [*Wang et al.*, 1996]. Even though they are usually optically very thin, they affect the earth radiation budget mainly by absorbing outgoing long-wave radiation [*McFarquhar et al.*, 2000]. Moreover, the sedimentation of ice particles dries the air as it enters the stratosphere through the tropical tropopause. Stratospheric water vapor has increased in the last decades until 2001 by about 1% per year [*Oltmans and Hofmann*, 1995]. This trend cannot be explained by increased water vapor production through methane oxidation alone [*Rosenlof et al.*, 2001; *Oltmans and Hofmann*, 1995]. Since the temperature of the tropical tropopause has rather decreased than increased in the passed decade [*Seidel et al.*, 2001], the trend of the stratospheric water vapor remains so far an unresolved problem with important impact on the radiative balance and the chemistry of the stratosphere. However, in the recent years from 2001 to 2004, unusually low water vapor concentrations were observed globally in the lower stratosphere which are in phase with variabilities of the tropical tropopause temperature [*Randel et al.*, 2004].

[3] A recent study by *Fueglistaler et al.* [2005] demonstrates that the water vapor concentration of the tropical lower stratosphere can be explained by the Lagrangian mean of the temperature minimum at the tropopause. This model study assumes that air which ascends from the troposphere into the stratosphere is readily dried to saturation pressure over ice at the coldest point of its trajectory. On the other hand observations of high supersaturation at the tropical tropopause are frequently reported [e.g., *Spichtinger et al.*, 2003b; *Jensen et al.*, 2005]. *Jensen et al.* [2005]

[1] Alfred Wegener Institute for Polar and Marine Research, Bremerhaven, Germany.
[2] Alfred Wegener Institute for Polar and Marine Research, Potsdam, Germany.
[3] Now at Leibniz Institute of Marine Sciences at the University of Kiel (IFM-GEOMAR), Kiel, Germany.
[4] Now at Department of Physics, University of Toronto, Toronto, Ontario, Canada.
[5] Faculty of Environmental Earth Science, Hokkaido University, Sapporo, Japan.
[6] Royal Netherlands Meteorological Institute, De Bilt, Netherlands.

0148-0227/07/2006JD007440$09.00

suggest that the freeze drying process takes place mainly in the western Pacific region where the tropopause is coldest, thereby ensuring the dryness of the stratosphere despite the high supersaturation necessary for cloud formation. Consequently, tropical cirrus are formed only in this region. This is somewhat contradictory to the observed high frequency of occurrence of high-altitude cirrus in other regions [*Wang et al.*, 1996; *Winker and Trepte*, 1998; *Immler and Schrems*, 2002].

[4] The exact nature of the transport of water vapor through the tropical tropopause remains a matter of active research. A pilot study held at Paramaribo, Suriname (5.8°N, 55.2°W) from September 2004 to March 2005 offered the opportunity to perform measurements at a tropical site over a longer period of time. Beside other instruments, the high-performance mobile Raman lidar MARL was run at the site from September to November 2004. As we will demonstrate in section 2, this system is capable of detecting extremely thin layers of solid particles at the altitude of the tropical tropopause. The large data set obtained during this campaign allows the determination of the frequency of occurrence of thin, subvisual, and extremely thin tropical cirrus. Owing to the Raman capabilities of the system, we were able to measure the so called lidar ratio, the ratio between the extinction and backscatter coefficients, of tropical cirrus clouds. The lidar ratio is an important parameter for lidars that do not have this capability, including future space based systems, in order to determine cloud optical depth and their radiative impact (section 3.1). For ten cases, lidar measurements were performed simultaneously with the launch of balloons carrying frost point hygrometers, which allow an accurate measurement of the humidity in the upper troposphere. In section 3 we present four such cases in detail in order to investigate the conditions at which tropical cirrus of different optical depths exist. The properties, formation mechanisms, and dehydration potentials of these clouds are then discussed in section 4 on the basis of trajectories which were calculated using a newly developed model. This model, as well as a standard trajectory model are used to test the hypothesis that air which is transported from the troposphere to the stratosphere is dried to the saturation vapor pressure at the lowest temperature it has experienced. Finally a discussion (section 4) of the results and a summary (section 5) are provided.

2. STAR Pilot Study

[5] In order to demonstrate the capabilities and test the limits of ground based measurements in a tropical environment a pilot study was performed in the framework of the EU project STAR (Support for Tropical Atmospheric Research, see http://www.knmi.nl/samenw/star/). The lidar, a Fourier Transform Infrared Spectrometer (FTIR), a sun photometer, and a UV radiometer were installed at the site of the "Meteorologische Dienst Suriname (MDS)" in Paramaribo (5.8°N, 55.2°W) and measurements were performed from 27 September 2004 to 16 November 2004. This observation period was during the local long dry season when the intertropical convergence zone (ITCZ) lies to the North of Suriname, over the Atlantic. A second campaign followed in February/March 2005 during the short dry season, when the ITCZ is further south over the Amazon basin. Daily radiosonde launches provided temperature, pressure and wind profiles and occasionally during night time, a frost point hygrometer of the type "Snow White" was launched that allows a precise determination of the water vapor profile. The behavior of this sonde in the cold upper tropical troposphere has been studied by *Vömel et al.* [2003], *Fujiwara et al.* [2003b], and *Verver et al.* [2006], who have found good performance up to at least 16 km altitude. This study uses the Snow White data up to 18 km that have passed the quality check suggested by *Fujiwara et al.* [2003b]. In this work we concentrate on the lidar and Snow White data acquired during the first pilot study from September to November 2004.

2.1. Lidar Measurements of Tropical Clouds

[6] The Mobile Aerosol Raman Lidar (MARL) of AWI is a backscatter lidar using a Nd:YAG laser which has an output power of 350 mJ at 532 nm and 355 nm at 30 Hz repetition rate. The lidar signals are detected by means of a 1.1 m diameter quasi-Cassegrain telescope with a field-of-view of 0.4 mrad and a 10-channel detection system that uses analog and single photon counting data acquisition simultaneously [*Schäfer et al.*, 1997]. The backscatter profiles are measured at 532 nm and 355 nm separated by polarization. Raman signals of nitrogen and water vapor are excited at 355 nm and are detected at 387 nm and 407 nm, respectively. The nitrogen Raman signal excited at 532 nm is detected at 607 nm. The temporal and vertical resolutions are 140 s and 7.5 m respectively.

[7] Layers of particles in the atmosphere are detected in the lidar signals by the increase in backscattering they induce. The automatic cloud detection algorithm reports the presence of a cloud base when the slope of the modified backscatter signal represented by the function $R'(z)$ is greater than 3 times its noise. $R'(z)$ is defined by

$$R'(z) = \frac{d}{dz} \ln \frac{P(z)}{P_{Ray}(z)} \tag{1}$$

where $P(z)$ is a measured lidar signal as a function of the altitude z and P_{Ray} is a synthesized purely molecular lidar signal. The noise of that function is derived from Poisson statistics of the photon-counting signals (or photon-counting equivalent signal when using the analog detection) and are calculated using error propagation theory. Typical values for a lidar signal integrated over 140 s (4096 single shots) for $\Delta R'$ are 1 km^{-1} and 5 km^{-1} for the parallel and perpendicular polarizations, respectively. The minimal thickness of a cloud required for detection was set to 30 m (4 bins). This translates to a minimum integrated backscatter at 16 km altitude of 2×10^{-7} sr^{-1} and 1×10^{-8} sr^{-1} and, using an extinction to backscatter ratio S of 30 sr, to a minimum detectable optical depth (OD) of 6×10^{-6} and 3×10^{-7} based on the parallel and perpendicular signals, respectively. Since most observed clouds were thicker than 40 m, such low values hardly ever occur. A layer detected in this way was classified as a tropical cirrus (TC) when its base is above 12 km and it showed significant depolarization. This was the case when a volume depolarization of more than 2% at 532 nm was measured which is significantly more than the depolarization of molecular scattering of 1.44% [*Behrendt and Nakamura*, 2002]. A

depolarization of 2% is enough to indicate the presence of nonspherical particles of sufficient size ($r_{eff} > 0.3$ μm [*Mishchenko and Sassen*, 1998]).

[8] These calculations demonstrate the extremely low detection limit of our lidar system, while the high value of the discrimination level ($3 \times \sigma$) ensures a small false alarm rate of the automatic cloud detection scheme. The optical depth of a cloud can be measured directly by virtue of the nitrogen Raman scattering. Using again equation (1) and putting the Raman signal in place of the elastic signal, delivers double the extinction [*Ansmann et al.*, 1992]. The Raman errors at 16 km at 532 nm and 355 nm are typically 2×10^{-3} m^{-1} and 1×10^{-3} m^{-1}, respectively, on the basis of 60 min averages. The optical depth of a cloud layer can be retrieved by integrating the extinction over the altitude range of the cloud. Typically, the uncertainty of the direct measurement of the optical depth is about 0.005, more or less independent of the actual optical depth of a cloud. Assuming a constant extinction-to-backscatter ratio S throughout a cloud layer, this ratio (often termed lidar ratio) can be determined for clouds with an optical depth larger than 0.05 with an accuracy of about 10% or better. For clouds optically thinner than 0.05, the optical depth and the lidar ratio cannot be measured. However, one can still derive a reasonable estimate for the optical depths of thin clouds by multiplying the integrated backscatter coefficient by the mean value of S obtained for the thicker clouds.

[9] For all measurements reported here, the so-called "color index" which describes the wavelength dependence of the backscatter coefficient, was around zero. This means that little information on the particle size can be retrieved from the lidar data. In order to obtain some information on particle number and condensed mass, an assumption on the effective particle radius needs to be made. Remote sensing and in situ measurements indicate that for thin cirrus an estimate of 10 μm for the effective radius is reasonable [*Thomas et al.*, 2002], while for extremely thin cirrus a value of 5 μm is more appropriate [*Peter et al.*, 2003]. Mie theory was used to translate the measured backscatter coefficient into a particle number concentration and an ice water content (IWC) on the basis of these assumptions on the effective radii. Since no correction for the asphericity of the particles was made, the quantities derived from these assumptions should be considered as rough estimates only.

2.2. Trajectory Model

[10] In order to investigate the source regions and possible formation mechanisms of tropical cirrus clouds a transport model was used which was recently developed at AWI. To avoid the noisy [*Manney et al.*, 2005] and high [*Scheele et al.*, 2005; *Meijer et al.*, 2004] vertical velocities of assimilation systems in quasi-isentropic trajectory calculations, diabatic heating rates were used to determine the vertical transport in the stratosphere. The heating rates were derived from a stand-alone version of the ECMWF's radiative transfer model [*Morcrette et al.*, 1998], using operational ECMWF's temperature, ozone, water vapor, cloud cover and cloud content fields every 6 hours as meteorological input. The quasi-isentropic trajectories were calculated for selected periods during September to November 2004 also using the operational ECMWF fields on 60 vertical levels and a spectral truncation of T511 (L60T511). The horizontal wind and temperature fields were then interpolated on T106 resolution and on $2^\circ \times 2^\circ$ Gaussian grid prior to the trajectory calculations.

[11] The newly developed trajectory tool is described in more detail by [*Tegtmeier*, 2006] using three-dimensional horizontal wind and temperature fields from ECMWF and the off-line derived heating rates all on a regular $2^\circ \times 2^\circ$ grid spacing. The trajectory model was run with a time integration step of 20 min, while the output was reduced to a 6 hour spacing. We refer to these trajectories as AWI trajectories hereafter. The trajectory model was originally developed in order to study vertical transport in the polar stratosphere. However, as we demonstrate, it produces meaningful results also in the tropical tropopause region, above the level of zero net radiative heating which in the tropics is found at about 15 km altitude [*Gettelman et al.*, 2004].

[12] During the time period when lidar measurements were available, backward and forward trajectories were started over Paramaribo on a 6 hour time grid (0000, 0600, 1200, 1800 UT) and on isentropic levels between 350 and 400 K. This yielded a large set of 1260 trajectories, which enable us to conduct a statistical analysis of the data. Additionally, backward trajectories were calculated for the exact time of the concurrent balloon and lidar soundings which are described in detail in section 3.2.

[13] For comparison, standard trajectories based on ECMWF horizontal and vertical winds were retrieved for the case studies, using the trajectory service of the British Atmospheric Data Centre (BADC, http://badc.nerc.ac.uk/). These trajectories are referred to as BADC trajectories hereafter.

[14] The relation between relative humidity, cloud formation, and dehydration was studied by a simple scheme that derives the humidity in the TTL from the temperature history of the trajectories in analogy to the assumptions used by *Fueglistaler et al.* [2005] and *Bonazzola and Haynes* [2004]. We assumed, that the relative humidity above ice (RH_I) was 100% at the beginning of the trajectory 14 days earlier ($t = -14d$). When the air is cooled upon ascent the relative humidity increases and eventually exceeds 100%. We further assumed that clouds effectively dehydrate the air by the sedimentation of ice particles and limit RH_I to 110%. We chose this value in order to make the numerical calculation stable and realistic without significantly interfering with the initial assumption of ice formation at ice saturation. Also this value provided the best correlation with the measurements. As the air ascends and cools, it will dehydrate more and more, whereas the water vapor mixing ratio (WVMR) remains constant in case of descending motion (i.e., increasing temperature and pressure). In all cases where the air trajectory encountered a temperature minimum $T_{\min}$ the water vapor content of the air parcel is determined by 110% of the saturation mixing ratio $n_{\min}$ at this point:

$$n_{\min} = 1.1 \cdot \frac{v(T_{\min})}{p_{\min}} \tag{2}$$

where $v(T_{\min})$ is the saturation vapor pressure above ice calculated by Sonntag's formula [*Sonntag*, 1994] and $p_{\min}$ is

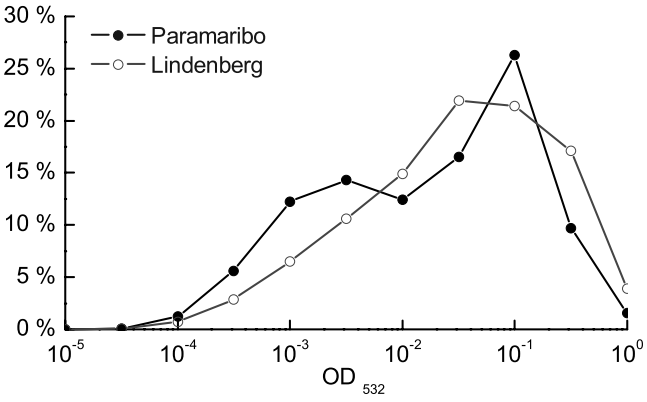

Figure 1. Relative frequency distribution of the optical depth of tropical cirrus (dots) and midlatitude cirrus (open circles).

the pressure at this point. The relative humidity RH_I^{traj} at the reference point ($t = 0$) of the trajectory is then given by:

$$RH_I^{traj} = \frac{n_{\min} p_0}{v_0} \tag{3}$$

where p_0 and v_0 are the pressure and the saturation vapor pressure above ice at $t = 0$, respectively. In all cases where the air temperature reaches its minimum at $t = 0$ the air will be (super-)saturated with $100\% < RH_I^{traj} < 110\%$.

3. Observations

[15] Overall, 480 hours of lidar observations were obtained at Paramaribo, mainly during night time, since the low zenith angle of the sun around noon thwarted measurements during that time. This study focuses on the first intensive campaign from 25 September 2004 to 16 November 2004 where 410 hours of lidar measurements were acquired. During 37 nights measurements were taken for more than 4 hours. Thirty-three of these nights were fully cloudy as far as cirrus occurrence was concerned. During three nights clouds were detected about half of the time and only on two nights there were almost no clouds detected in the upper troposphere. Overall, cirrus was present in 88% of the time. If we consider only clouds with a base height above 12 km the cloudiness was still 81%.

[16] The mean optical depth of these clouds was 0.04, around the visibility threshold. Figure 1 shows the relative frequency of occurrence of the optical depth (OD) of tropical cirrus. This function can be characterized by a bimodal distribution. Besides the main peak around 0.1 there is a second mode occurring around 0.003. Comparing these with results from measurements of cirrus at midlatitudes obtained during a previous campaign, it became evident that the probability of encountering extremely thin cirrus in the tropical upper troposphere was clearly enhanced relative to the midlatitudes. This might be explained by an enhanced life time of these thin tropical cirrus compared to their midlatitude counterparts. The bimodal shape of the distribution in Figure 1 suggests a discrimination between two types of cirrus clouds in the tropics: thin cirrus (TTCi) with optical depth between 0.03 and 1 which are usually visible to the bare eye and subvisual cirrus (SvCi) with optical depth below 0.03. Layers of particles with optical depths below 10^{-3} are termed extremely thin tropical cirrus (ETTCi). About 20% of the clouds detected by the lidar were of the extremely thin type, 40% were subvisual and another 40% were thin cirrus.

[17] Figure 2 shows the distribution of the base height of clouds with different optical depths. Visible cirrus occur most often around 12 km. At higher altitudes clouds become optically thinner. Subvisual cirrus were typically located between 14 and 16 km. Extremely thin cirrus (ETTCi) with optical depth below 10^{-3} were mostly observed around 17 km. The cold point tropopause was usually located at this altitude (dashed line).

3.1. Extinction-to-Backscatter Ratio

[18] The extinction-to-backscatter ratio or lidar ratio S is an important parameter for the inversion of lidar signals for instruments that do not have a Raman channel. Future space based lidars, such as CALIPSO (Cloud-Aerosol Lidar and Infrared Pathfinder Satellite Observations, http://www-calipso.larc.nasa.gov/), depend on such a parametrization that may vary with location and cloud type. Recently, *Whiteman et al.* [2004] provided measurements of S at a subtropical site (Andros, Bahamas, 24.7°N, 77.75°W), but no direct measurements are yet available from the deeper tropics and south of the intertropical convergence zone (ITCZ). The STAR pilot study therefore provided the rare opportunity to perform Raman lidar measurements in these regions. The values retrieved from the data measured at Paramaribo are compared to those from a previous campaign at Lindenberg (53.2°N, 14.12°E) in Figures 3a and 3b.

[19] We find that tropical cirrus have systematically a higher lidar ratio than midlatitude cirrus. This is shown in Figure 3a where the lidar ratio is plotted against the optical depth. Except for optically thick clouds the lidar ratio (at 355 nm) measured at Paramaribo is with a mean value of 26 ± 7 sr higher by 50% than the value of 16 ± 9 sr which was obtained from the data from Lindenberg where the variability is also higher. For tropical cirrus the lidar ratio tends to increase with decreasing optical depth while the opposite trend occurs for thin midlatitude cirrus. While no

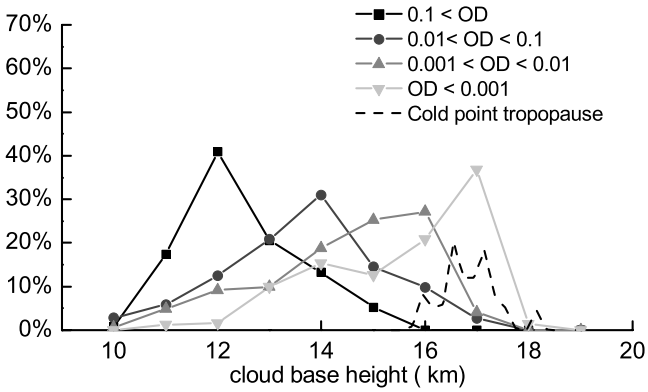

Figure 2. Relative frequency distribution of the base height of clouds with different optical depths as indicated. The solid line shows the altitude distribution of the cold point tropopause.

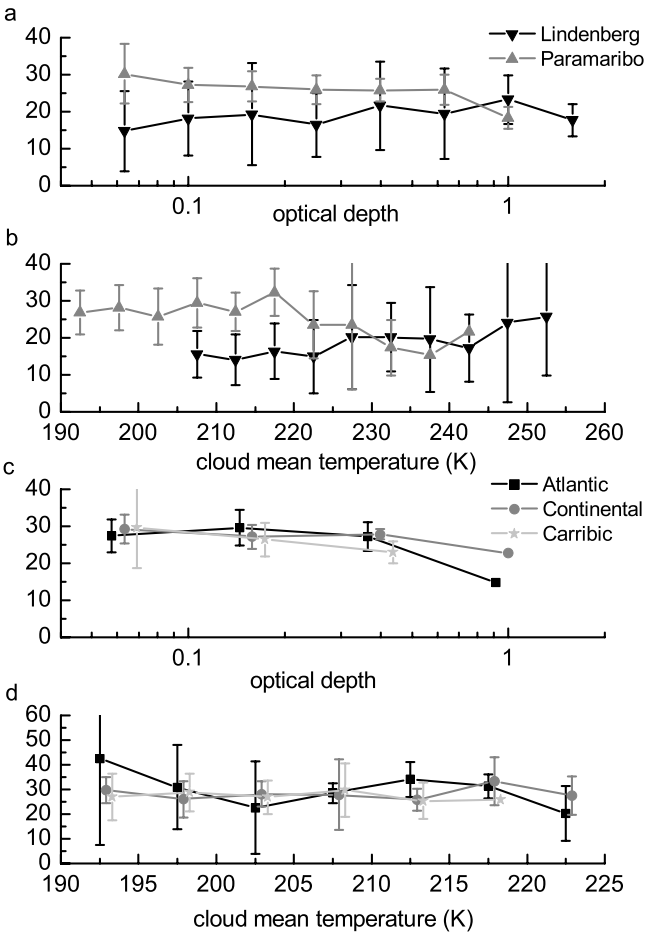

Figure 3. Extinction-to-backscatter ratio S of (a and b) cirrus clouds observed at different latitudes and (c and d) of tropical cirrus with different source regions (see text for details). Figures 3a and 3b compare tropical cirrus observed at Paramaribo to midlatitude cirrus observed with the same instrument in summer 2003 at Lindenberg/Germany. Plotted is S as a function of the cloud optical depth (Figures 3a and 3c) and the cloud mean temperature (Figures 3b and 3d).

difference between tropics and midlatitudes is obvious for warmer clouds, it becomes significant for colder clouds with $T < 220\ K$ (Figure 3b). The lidar ratio depends on microphysical properties of the cloud particle like size, shape, and refractive index. However, there is no simple relationship between these parameters and the lidar ratio. The reason for the differences between tropical and midlatitude cirrus is currently unknown.

[20] To investigate this further, the Paramaribo data set was regrouped into three subsets according to the origin of corresponding AWI backward trajectories. We found three different flow patterns to be representative in the upper troposphere: (1) flow from the north or northeast originating from the Atlantic; (2) flow from the northwest, from the Caribbean; and (3) flow from west to southwest from the South American continent. Figures 3c and 3d show the lidar ratio as function of the optical depth and temperature, respectively, for theses three subsets. There is no obvious difference, suggesting that the properties of tropical cirrus do not strongly depend on the origin of the air mass.

[21] The availability of the Snow White frost point hygrometer during the pilot study allowed a direct comparison of cirrus detection with a lidar and humidity measurement by the frost point hygrometer. Figure 4 shows histograms for the relative humidity inside and outside of cirrus clouds. Only 5% of the cloud free regions are detected as supersaturated. Inside cirrus the relative humidity peaks around 100%. High supersaturations ($RH_I >$ 120%) are rarely detected by this instrument.

3.2. Case Studies

[22] To study the occurrence of cirrus in the upper tropical troposphere in more detail, four cases are presented in this section.

3.2.1. A Typical Case: 21 October 2004

[23] The first case, from 21 October 2004 (Figures 5a–5e), shows a typical situation, which is observed frequently in the tropics: during this night, cirrus was detected at various altitudes from 10 km up to 17 km. A balloon carrying a Snow White sonde was launched at 0743 UT (0443 local time) and reached the tropopause at 16.5 km about 1 hour later. Figure 5c presents the relative humidity above ice (cyan) and Figure 5d the temperature (red) measured by this probe along with lidar and model results.

[24] The black line in Figure 5d indicates the backscatter ratio (532 nm) measured by the lidar averaged from 0807 UT to 0840 UT, the time period when the balloon probed the upper troposphere. During this period there were several cloud patches detected between 10 and 14 km.

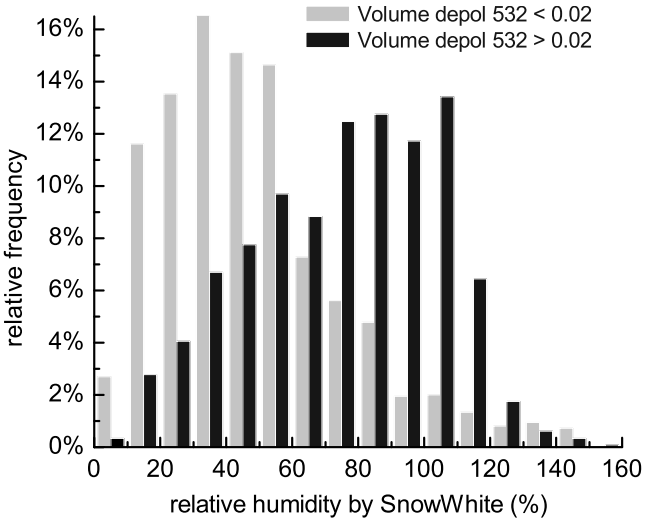

Figure 4. Histogram of the relative humidity above ice measured by the Snow White sonde in the upper troposphere (12 km < h <18 km) divided into two cases where the lidar detected a cloud (depolarization >2%, solid) in the corresponding altitude range or not (shaded). This analysis is based on the maximal altitude resolution of the lidar (7.5 m) and a 20 min temporal resolution with a time delay Δt between radiosonde launch time and the starting time for the lidar averaging period of 0.5 $h < \Delta t < 1\ h$. Thus the lidar data was acquired in about the same time period when the radiosonde crossed the altitude range 12 km < h <18 km.

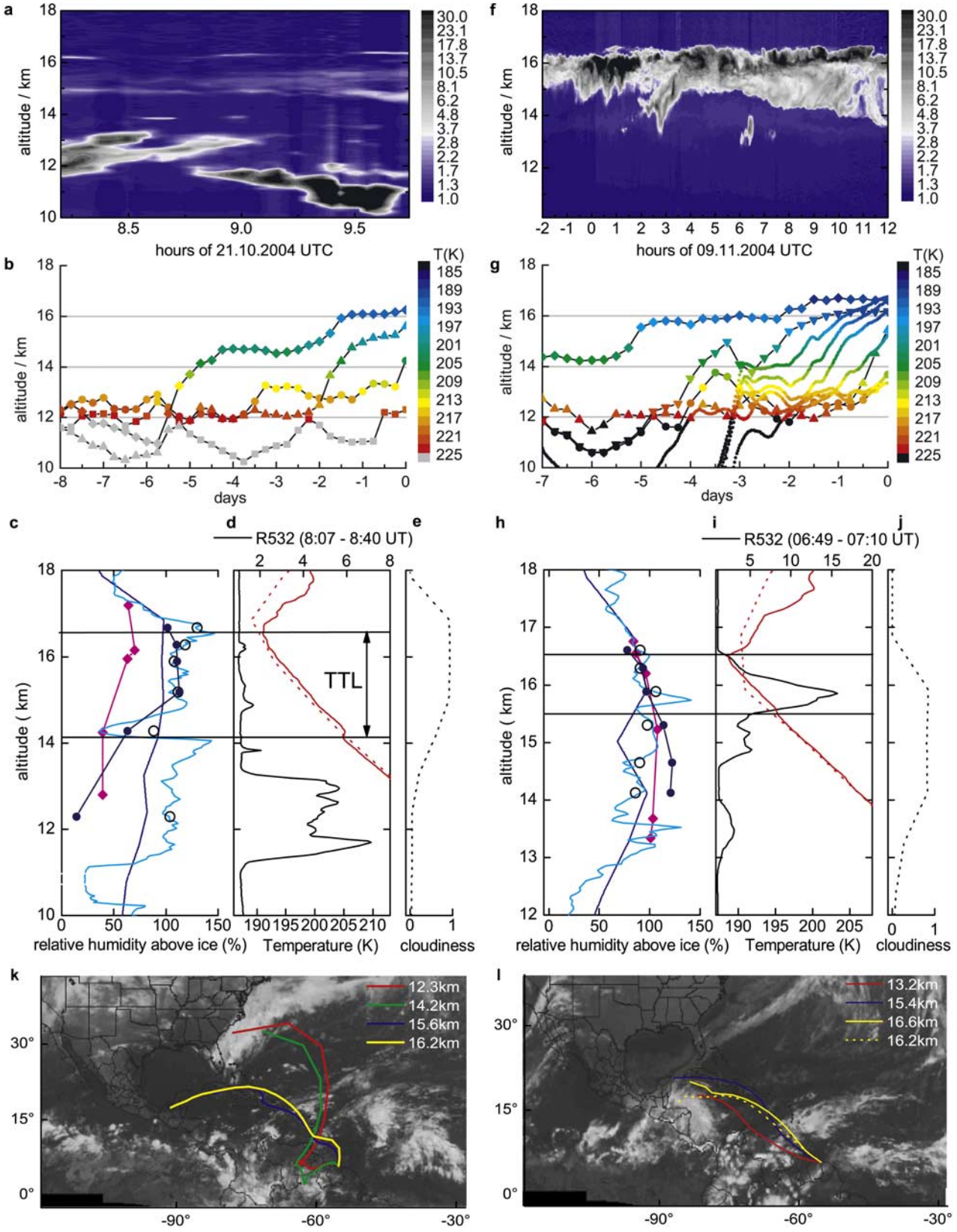
a
altitude / km
hours of 21.10.2004 UTC
30.0
23.1
17.8
13.7
10.5
8.1
6.2
4.8
3.7
2.8
2.2
1.7
1.3
1.0
f
hours of 09.11.2004 UTC
b
T(K)
185
189
193
197
201
205
209
213
217
221
225
days
g
c
d
e
R532 (8:07 - 8:40 UT)
TTL
altitude (km)
relative humidity above ice (%)
Temperature (K)
cloudiness
h
i
j
R532 (06:49 - 07:10 UT)
k
12.3km
14.2km
15.6km
16.2km
l
13.2km
15.4km
16.6km
16.2km

Figure 5

These rather thick cirrus clouds had optical depths around 0.1 and occurred in the temperature range of 210 and 230 K. The upper boundary of the layer containing these clouds was clearly marked by a thin ice layer and an upper tropospheric inversion at 14 km (Figure 5d). The trajectories trace the corresponding air mass in the first place back to the western Amazon region where it most likely was injected by deep convection less than a day earlier (Figure 5k, red trajectory and Figure 5b, squares).

[25] The backscatter coefficient of these clouds determined from the lidar data is around 3×10^{-6} m^{-1} sr^{-1}. Assuming an effective radius of the cloud particles of 10 μm, these ice clouds contain about 100 particles/L. The ice water content (IWC) is on the order of 0.3 mg/m^3. Given a concentration of water vapor of about 7 mg/m^3 as measured by the probe, about 5% of the total available water is condensed in the cloud particles.

[26] A thin inversion layer about 1 to 3 km below the cold point tropopause is a typical feature of the upper tropical troposphere [*Fujiwara et al.*, 2003a; *Immler and Schrems*, 2002]. We would like to refer to the layer above 12 km and below the temperature inversion as the upper troposphere (UT), while we use the term "tropical tropopause layer" (TTL) for the altitude range between the upper tropospheric inversion (UTI) and the cold point tropopause (CPT). This definition differs somewhat from descriptions given elsewhere in the literature, where the lower TTL boundary is defined as the minimum in the potential temperature lapse rate [*Gettelman and Forster*, 2002] or the level of zero net radiative heating [*Gettelman et al.*, 2004]. A detailed analysis of the dynamical features of the TTL at Paramaribo, which also explains the existence of an UTI, was carried out in a companion study by *Fortuin et al.* [2007].

[27] In contrast to the origin of the air in the UT, the air in the TTL came in from the northwest (Figure 5k, blue and yellow). The steep slopes at $t = -2$ of the upper two trajectories in Figure 5b indicates an influence of deep convection on the TTL. At that time the air moved across the ITCZ which stretched from South-Central America to Puerto Rico and into the Atlantic Ocean (Figure 5k). Thin ice clouds with optical depths around 0.003 reside in this layer. Assuming an effective radius of 5 μm, these subvisual cirrus clouds contain about 40 particles/L with an IWC of 0.02 mg/m^3, meaning that only about 1% of the total water is condensed in these particles.

[28] The uppermost trajectory, shown in Figure 5b, corresponds to the air mass at the cold point tropopause and indicate that this air has gradually been lofted in the last 5 days. Extremely thin cirrus (OD < 10^{-3}) exists right below the cold point (Figure 5d, 16.2 km).

[29] The AWI trajectories indicate that the closer a tropospheric air mass is to the cold point tropopause, the longer it has been dwelling in the upper troposphere. In contrast, cirrus clouds that occur below the UTI around 12 km altitude are more or less a consequence of convective outflow. At higher altitudes, in the TTL, subvisual cirrus occurs, obviously created and/or sustained by slow ascent in an air mass of an age on the order of days. This picture agrees well with the results from *Folkins et al.* [1999], who showed that there is a barrier to vertical mixing at about 14 km which corresponds to the level of neutral buoyancy of air with boundary layer properties. Above this level, the air in the transition layer is characterized by slow, large-scale ascent.

[30] The Snow White sonde data indicate that the air in the UT and in the TTL are moist with relative humidities above ice (RHI) larger than 95%. High supersaturation occurs in sharp peaks at the CPT at 16.5 km and just below the UTI at 14 km. Inside the UT cloud the relative humidity above ice varies in the range from 95% to 110%, while inside the TTL cirrus between 13.8 km and 14.8 km values of 130% are reached.

[31] The humidity modeled using the AWI trajectories shown in Figure 5b is plotted in Figure 5c as dark blue dots. The average values of the Snow White measurement within the altitude ranges that correspond to each of the trajectories are marked in black circles. The agreement between the modeled relative humidity and the measurement inside the TTL, which is marked by horizontal lines, is remarkable. Also, the extremely dry layer right above the UTI is captured by the model: according to the corresponding trajectory, the air parcel had reached high altitudes and low temperatures of below 200 K 12 days earlier and evidently the air was efficiently dehydrated at that time. This event occurred in the central Pacific, near the equator. Below the TTL, the AWI model fails to predict the relative humidity correctly. Since this model does not account for convection explicitly, this disagreement suggests that the moist air observed between 11 and 14 km was deposited by convective transport, in agreement with our previous remark

Figure 5. Measurements and trajectory analysis of clouds in the TTL from (a–e) 21 October 2004 and (f–j) 9 November 2004. Figures 5a and 5f show the backscatter ratio at 532 nm as a function of time and altitude. Figures 5b and 5g display the altitude of various backward trajectories started 0600 UT on each day. The temperature at each point is color coded. The thin lines (only 9 November) indicate BADC trajectories, while the thicker symbols refer to AWI trajectories. Figures 5c and 5h show the relative humidity as measured by the Snow White sonde (RH_I^{SW}, solid cyan line) launched at 0743 UTC (Figure 5c) and 0619 UTC (Figure 5h), from the ECMWF model (0600 UT, 6°N, 52°W, solid blue line) and retrieved from the AWI and BADC backward trajectories (dark blue and pink dots, respectively). The black circles indicate the mean value of RH_I^{SW} within the altitude range covered by the corresponding AWI trajectory. Figures 5d and 5i show the temperature profiles measured by the radiosonde (red) and from the operational ECMWF analysis data (dashed black line). The black line indicates the backscatter ratio at 532 nm at the time of the balloon launch (+60 min ±10 min). The dotted line in Figures 5e and 5j depicts the ECMWF cloudiness. The horizontal lines indicate the altitude range of the TTL. AWI backward trajectories for (k) 6 days and (l) 3.2 days on top of a satellite image from 20 October 2004, 1145 UT (Figure 5k) and 5 November, 2345 UT (Figure 5l). The GOES infrared (11 μm) images were retrieved from the Unisys server (http://weather.unisys.com/satellite/). The altitude of arrival is indicated in the top right corner. The dashed line on Figure 5l shows a BADC trajectory for comparison.

that cirrus in the UT region are mostly formed in the outflow of deep convection.

[32] The blue curve in Figure 5c shows the humidity profile of the operational ECMWF analysis. It also indicates a moist TTL, but the relative humidity does not reach the high values measured by the sonde, nor is the dry layer at 14.2 km reproduced. The pink diamonds depict the modeled relative humidities based on BADC trajectories. Obviously the AWI trajectories with vertical motion based on diabatic heating rates yields a much better representation of the upper troposphere's humidity. The thin dotted line in Figure 5e shows the cloudiness represented in the ECMWF operational data. The model fails to predict the cirrus in the upper troposphere but it predicts a cloudy TTL in good agreement with the observations.

[33] In the following section three cases are analyzed where three different types of cirrus were present in the TTL: thin visible cirrus, subvisual cirrus, and, almost, no clouds at all.

3.2.2. Thin Visible Cirrus: 9 November 2004

[34] On 9 November 2004 cirrus (Cs) with optical depth around 0.1 was observed throughout the night. At 0619 UT (0319 local time) a Snow White probe was launched from the MDS site. The results from the lidar, the radiosonde and the AWI trajectory calculations are shown in Figures 5f–5j. The backscatter coefficient peaks at 6×10^{-6} m^{-1} around 16 km altitude and is approximately as high as the one of the cirrus in the UT on 21 October 2004. Assuming a particle effective radius of 5 μm for this cirrus (since it is inside the TTL), the ice water content of the cloud reaches up to 0.3 mg/m^3, meaning that in the supersaturated environment 30% of the available water is condensed. If the radius was 10 μm this number goes up to 60% (the IWC scales about linearly with radius when the backscatter coefficient is kept constant). This newly formed, high-altitude cirrus contains a large amount of the available water and therefore can very effectively dehydrate the air. The forward trajectory calculations (not shown) demonstrate that the upper part of the cirrus continues to rise and that the air is transported into the stratosphere. Assuming that the air was dehydrated to saturation vapor pressure, the air mass going through the cold point at Paramaribo will contain 3 ppm of water. On its way eastward however, this air mass encounters another temperature minimum of 187 K around the Horn of Africa where the water content is then lowered to 2.66 ppm (not shown).

[35] The relative humidity derived from the temperature history RHI_I^{traj} of the air parcel matches the measured values well in the TTL. The BADC trajectories (diamonds in Figure 5h) predict the measured humidity also in this case. The BADC trajectories (thin lines in Figure 5g) indicate that deep convection has transported air from below to an altitude of about 14 km about 3 days earlier. The satellite image from 6 November displayed in Figure 5l shows a convective zone in central America, which is likely to be the source region for this TTL air, since the air parcels were in this region and at that altitude at that time, according to both, the AWI and the BADC trajectories. While the air is advected toward Suriname, it rises by about 2 km. BADC and AWI trajectories agree in this respect (Figures 5g and 5l), but the details on how this vertical transport occurs are different.

[36] Interestingly, the temperature profile (Figure 5i) indicates a thin inversion at 15.6 km, just below the strongest peak in the backscatter. According to our definition, the upper part of the clouds is inside the TTL. The trajectories suggest the following scenario for the origin of this TTL cirrus: Moist air has been introduced three days earlier by the outflow from deep convection, and consequently rather thick clouds have formed, which contain a large amount of total water. Continuous lifting and cooling of the air maintain the clouds as it is advected toward our observation location. Since the relative humidity in the TTL is in mean only slightly above 100% in the TTL at Paramaribo according to the Snow White measurement, a significant amount of water must have been removed from the air parcel while it was cooled from about 206 K to 190 K. The saturation mixing ratios at these temperatures and corresponding pressures are 25 ppm and 3 ppm, respectively.

3.2.3. Subvisual Cirrus: 12 November 2004

[37] A large fraction of the clouds detected by the lidar at Paramaribo are subvisual (SvCi), i.e., have optical depths of 0.03 or less. These clouds often occur as an isolated layer at or close to the CPT above a thicker cirrus in the UT, as was the case of 21 October discussed above. In some cases the UT is free of clouds while there are still thin layers present at the CPT. Such SvCi occurred in the early hours of 12 November 2004 (Figures 6a–6e). The AWI trajectories indicate that the air mass holding the thin cloud were subject to steady ascent during the preceding two or three weeks (Figure 6b). The BADC trajectories (not shown) show a similar ascent, but because of larger temperature variation along the trajectories the modeled humidity is somewhat lower at the end (Figure 6c).

[38] The backscatter coefficient of the subvisual cloud is about 2×10^{-7} m^{-1} sr^{-1}, this corresponds to a particle number density of 30 L^{-1} provided the effective radius was 5 μm. The IWC according to this calculation was 0.013 mg/m^3 or 160 ppb equivalent gas phase volume mixing ratio. 17% of the precipitable water was condensed in the cloud, if the air was indeed as dry as measured by the sonde with RHI about 20% (Figure 6c). If the RHI was 100% the condensed water fraction is reduced to about 4%.

[39] The structure of the tropopause is very interesting: the temperature reaches a minimum at 16.7 km of 190 K and then stays more or less constant, i.e., between 190 and 191 K, for about 1 km. Exactly in this altitude range, the subvisual cloud is detected. Strictly speaking, this layer is within the stratosphere, i.e., above the temperature minimum.

[40] The temperature history of the trajectory, as well as the operational ECMWF analysis suggest that the relative humidity above ice is indeed about 100%. The ECMWF cloudiness (dotted line in Figure 6e) agrees well with the observations, since it also predicts high cloudiness in the corresponding altitude range. In contrast to these results, the Snow White sonde measures very low relative humidity. The internal data of the probe, like cooling current and housing temperature do not indicate a failure of the probe. Possibly, the balloon drifted away and happened to sampled a different, much drier air mass. This could explain the discrepancy between the Snow White and the lidar observations.

[41] Because of this problem with the Snow White sonde there remains considerable uncertainty as far as the humidity in the upper TTL is concerned. However, there is a

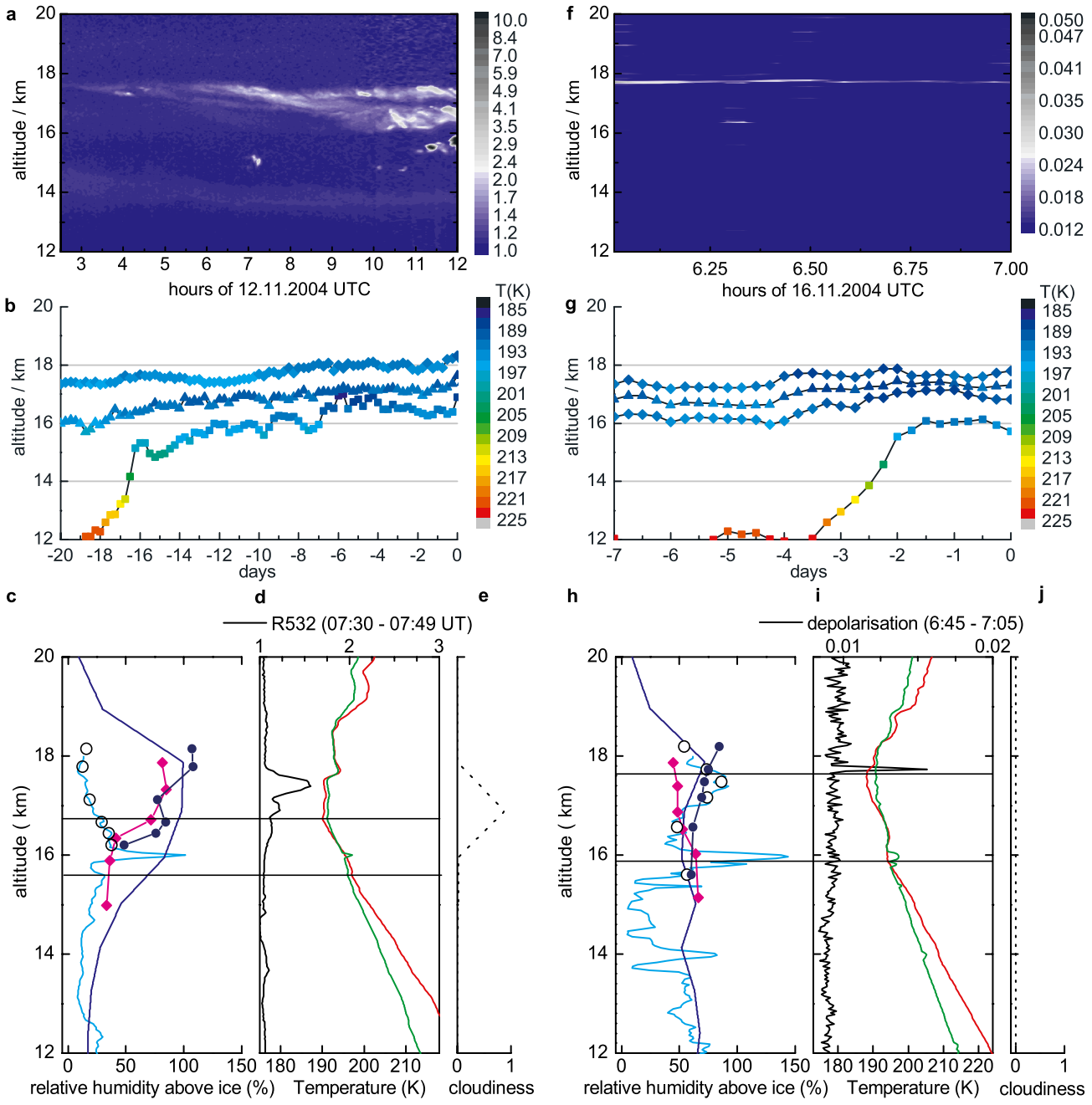

Figure 6. Same as Figure 5 but for (a–e) 12 November and (f–j) 16 November 2004, except for Figure 6f which shows the volume depolarization instead of the backscatter ratio at 532 nm, because the extremely thin layer of particles was not visible in the parallel backscatter. In Figures 6d and 6i the existence temperature of NAT is plotted in green. The balloons that measured relative humidity and temperature in Figures 6c, 6d, 6h, and 6i were launched at 0644 UTC (12 November 2004) and 0626 UTC (16 November 2004).

correlation between the saturation derived from the AWI trajectory and the observation of a cloud by the lidar at 17.8 km. This example shows that subvisual clouds do exist when the temperature of an air parcel reaches an absolute minimum and is consequently saturated ($RH_I^{traj} > 100\%$), if we ignore the Snow White data in this case. It is evident, that these clouds form in situ because of the long residence time of the corresponding trajectory in the TTL, which is on the order of weeks. During this time the temperature is not steadily decreasing but goes through local maxima. In the cases where we happened to observe air during one of these warmer periods we generally detect no clouds in the TTL, as we will demonstrate in the next example.

3.2.4. No Clouds: 16 November 2004

[42] In the early morning of 16 November 2004, the very last measurements of the first phase of the campaign were made. It is the only occasion where no clouds were detected in the tropopause region and humidity data from the Snow

White sonde are available (Figure 6h). The situation is partly comparable to the observation of 12 November discussed above. In both cases the UTI occurred at 16 km, the Snow White indicated a thin layer of high supersaturation in this region, however no cloud occurred there (Figure 6i). The cold point is found about 2 km higher and reaches temperatures as low as 188 K, but on 16 November no cloud was detected by the automatic routine described in section 2.1. In the TTL region neither the model output nor the Snow White data reached supersaturation. The air in the cold point region was, according to the AWI trajectories, at lower temperatures (187.5 K) about 2 days earlier, where it was obviously dried sufficiently to inhibit cloud formation later at higher temperatures. Our dehydration model, where we assumed a remaining water vapor content in the TTL according to equation (3), is confirmed by the Snow White measurement within ±15% (RH_I). The averaged difference between the predicted and the measured humidity is −3%; that is, the TTL is slightly drier than predicted by our assumptions.

[43] A visual inspection of the depolarization data of that day revealed that the tropopause region was not completely cloud free. A thin layer that was overlooked by the cloud detection algorithm, was present at the cold point at about 17.8 km (at 391 K potential temperature, Figures 6f and 6i) and was observed for about 1 hour. The backscatter coefficient of this particle layer was lower than 10^{-8} m^{-1} sr^{-1}. This corresponds to a particle number concentration of 1 L^{-1} (using $r_{eff} = 5$ μm) and an IWC of 5×10^{-4} mg/m^3. Even in this dry environment with a water vapor mixing ratio of 2.4 ppm, only 0.15% of the precipitable water was condensed. This calculation assumes that RHI was 60% as measured by the Snow White and that the cloud consisted of water ice. This layer is even thinner than the "ultrathin tropical cirrus" (UTTC) described by *Peter et al.* [2003] which was observed during an airborne campaign in the Indian Ocean. The fact that such a thin layer exists, suggests that there is no lower limit in terms of optical depth for the existence of depolarizing particles in this region.

[44] The extremely low fraction of condensed water, as well as the fact that the water measurement and the models indicate a subsaturated environment, suggest that this layer is not a simple water ice cloud. The observation of significant depolarization, on the other hand, indicates the presence of rather coarse solid particles with an effective radius above 0.3 μm [*Mishchenko and Sassen*, 1998]. Aerosol layers that are frequently observed by the lidar in the upper tropical troposphere generally do not depolarize. It is therefore more likely that the observed layer is a remnant of a cirrus cloud. We may assume that a subvisual cloud of similar properties as described in the previous section was present in this air mass some days ago, when the temperature was at its minimum. If the size of the particles of that cloud was reduced from 5 to about 1.5 μm by sublimation of water as the air slightly warms, an extremely thin cloud would remain at the tropopause with a backscatter coefficient as it was observed here. The questions remain, why would the cloud not evaporate completely in the subsaturated environment on the timescale of days? Probably, the low temperatures and the presence of trace species like HNO_3, HCl, HBr, or some organics even in small amounts could effectively slow down the evaporation rate [*Delval et al.*, 2003] and thus allow the detection of this extremely thin layer of particles. The green line in Figure 6i shows the existence temperature of Nitric acid trihydrate (NAT) according to a formula provided by *Hanson and Mauersberger* [1988] using a mixing ratio of 0.3 ppbV of HNO_3 in the TTL which seem realistic [*Jensen and Drdla*, 2002]. Accordingly, NAT can be stable around the cold point tropopause in the tropics. It is therefore plausible, that the observed layer of particles consists of NAT.

4. Discussion

4.1. Observational Results

[45] We found evidence for the occurrence of cirrus in 88% of all measurements. This number does not account for extremely thin layers of particles that were found at two occasions which were classified cloud free by the cloud detection scheme. The optical depth ranges from 1 to less than 10^{-5}. Inside the TTL about 90% of all clouds were subvisual ($OD < 0.03$). Compared to the midlatitudes, subvisual cirrus have an enhanced probability of occurrence in the tropics, proving that the TTL has favorable conditions to form and maintain thin cirrus clouds. According to our lidar observations, about 35% of the total volume of the TTL contained ice particles.

[46] The extinction to backscatter ratio (lidar ratio) with 26 ± 7 sr was found to be significantly larger for tropical cirrus with an optical depth >0.05 (for only which it can be measured) than the value determined in the midlatitude (16 ± 9 sr). *Whiteman et al.* [2004] measured a value of about 20 sr at 24°N in the subtropics indicating a systematic increase of the lidar ratio with decreasing latitude. This study is the only one that provides measurements of the lidar ratio in the deep tropics and should be of particular interest for future space based lidar missions that rely on a parameterization for the extinction-to-backscatter ratio in order to infer the optical depths of cirrus clouds.

[47] The reason for the shift of the lidar ratio with latitude is currently unknown. Differences in particle size and shape are possible explanations. Alternatively, a change of the properties of the interstitial aerosol that could also have a appreciable influence on the measured optical properties of optically thin ice clouds. We could not detect a relation between the origin of the cloud and the lidar ratio. Generally, the particles size is known to decrease with altitude [*Heymsfield*, 2003]. Since cirrus altitude increases with decreasing latitude this trend could explain the change in cirrus lidar ratio.

4.2. Trajectory Analysis

[48] We use a newly developed trajectory model to examine the origin and formation mechanisms of cirrus in the TTL. Generally we interpret rather thick clouds (OD about 0.1) that occur in the upper troposphere around 14 km as direct outflow from convectively active regions. Deep convection also feeds moist air into the TTL, which is dominated by slow ascent due to radiative heating. Thin cirrus forms and is maintained by adiabatic cooling on a timescale on the order of days. Higher cirrus tend to be optically thinner and the corresponding trajectories indicate longer residence times of the corresponding air mass in the TTL on the order of weeks. Details of the different cloud types are summarized in Table 1.

Table 1. Measured Properties of Tropical Cirrus[a]

			Cloud Top					Cold Point	
Date	Time, UT	Cloud Type	Altitude, km	Temperature, K	IWC (r_{eff} = 5 μm), mg/m^3	Optical Depth	RHI_{max}, %	Altitude, km	Temperature, K
9 Nov 2004	0600	TTCi	16.7	190 (190)	0.3	0.1	144 (97)	16.5 (16.9)	187 (190)
12 Nov 2004	0600	SvCi	17.7	194 (187)	0.01	3×10^{-3}	26 (99)	16.7 (17.9)	190 (187)
16 Nov 2004	0600	ETTCi	17.8	190 (190)	0.0004	1×10^{-6}	84 (70)	17.6 (17.8)	188.1 (190)

[a]Numbers in brackets are derived from ECMWF operational analysis.

[49] The case studies presented above indicate a correlation between the occurrence of clouds and the temperature history of the air parcels reflected in the calculated relative humidity. In order to study this more generally, we have calculated a large set of backward trajectories for the entire STAR pilot study period. At each ECMWF model level of the upper troposphere a trajectory was calculated and those were selected that start in the TTL according to the temperature profile measured by the temporally nearest radiosounding. Figure 7 shows the relative humidity calculated for the trajectories in the way described above (equation (3)) versus the maximum depolarization detected by the lidar in the corresponding altitude (~1 km) and time range (±3 hours). The result shows an obvious correlation between the water content simulated by the AWI trajectory model and the detection of clouds. In almost all cases (95%) where the air according to the trajectory should be saturated, ice particles were observed by the lidar. In a very large fraction (approximately 80%) of cases where the air has experienced significantly lower temperatures before arriving at Paramaribo, leading to a clearly subsaturated air with $RH_I^{traj} < 80\%$, no clouds were detected. There is an intermediate range with $80\% < RH_I^{traj} < 100\%$ where clouds tend to be present while the air was on average subsaturated. This could be due to various reasons: incomplete dehydration, rehydration by injections from the UT or by sedimenting particles from above or other processes which are not considered in our simple model.

[50] The fact that about 70% of the cloud observation can be explained by the humidity evolution of the AWI trajectories implies three important conclusions:

[51] 1. The trajectory model using diabatic heating rates describes the transport in the TTL very well.

[52] 2. Where there is saturation in the TTL, there is ice. It needs to be emphasized that little can be learned about the cloud formation conditions themselves from this finding. In particular nothing can be deduced about the supersaturation that is necessary to form the clouds. By definition, the method does not allow for high supersaturation and the cloud formation might occur on much smaller scales than considered in this analysis. A much higher temporal resolution of the meteorological input data would be needed for this purpose which is currently not available. This is also reflected in the measurements; that is, on 9 November the mean humidities as measured by the Snow White in the two ECMWF altitude bins of the TTL between 14.6 km and 16.6 km was 105% and 90% while a maximum of 140% occurred around 15.8 km, which is presumably a region of intense particle formation. High supersaturation occurs generally in thin layers [*Spichtinger et al.*, 2003a] and is therefore smoothed out by this analysis. Therefore our result is not in contradiction to reports of high supersaturations measured in situ inside [*Heymsfield et al.*, 1998] and outside of cirrus [*Jensen et al.*, 2005]. Still, one conclusion on cloud formation can be drawn from our observations: Whatever it takes to form clouds in the TTL does not prevent them from forming on the long run, once that ice saturation is exceeded. The timescales where supersaturation exists without the presence of a cloud should be short compared to the life time of the cloud that will eventually form. This result of the trajectory analysis is supported by the comparison between Snow White data and lidar observation (Figure 4) which shows only an insignificant amount of supersaturation of a few percent outside of clouds.

[53] 3. The fact that no clouds are observed when $RH_I^{traj} < 80\%$ demonstrates, that the air parcel "remembers," that it went through a significant cold trap earlier along its way through the TTL. It follows, that significant dehydration occurs in these events and that subsequent rehydration does generally not occur. A more precise quantification of the efficiency of this dehydration goes beyond the possibilities of this method. However, we find reasonable agreement

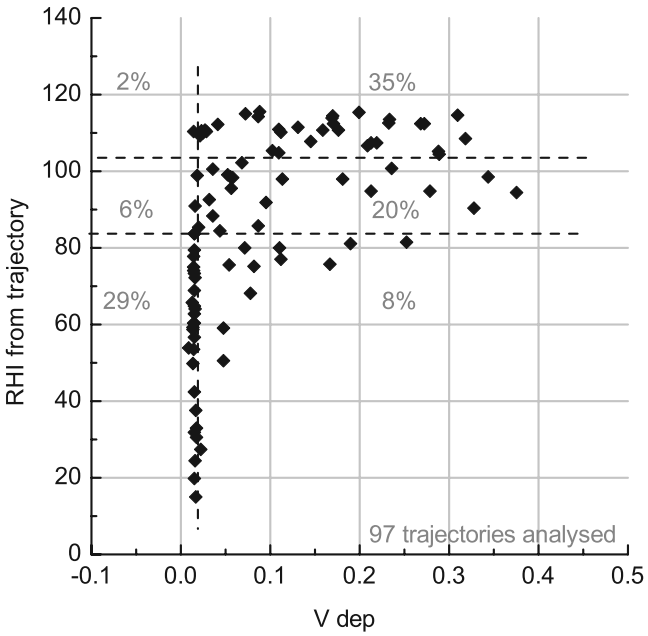

Figure 7. Relative humidity derived from the AWI trajectory temperature history versus the maximum depolarization measured by the lidar at the corresponding time and altitude. The trajectories were calculated for the entire STAR pilot study time period and the altitude range of the TTL. The dashed lines mark the significance level of clouds on the x axis and the range for saturation, modest subsaturation and clear subsaturation on the y axis. The numbers indicate the fraction of data points that fall in the different fields marked by the dashed lines.

between the assumption of efficient dehydration (RH_I^{max} = 110%) and measurements of the humidity in dehydrated TTL air masses by the Snow White sonde (Figure 6h). This supports the hypothesis of the dehydration of air entering the stratosphere to approximately the saturation pressure at the temperature minimum of its trajectory [*Fueglistaler et al.*, 2005].

4.3. Extremely Thin Tropical Cirrus (ETTCi)

[54] We provide evidence for the occasional presence of extremely thin layers of solid particle at the cold point tropopause. Such layers were observed on 11 November (not shown) and 16 November 2004 at about 17.8 km. In both cases operational ECMWF data, trajectory analysis and, where available, frost point hygrometer measurements indicate a humidity below ice saturation. On 11 November this layer was observed steadily for 4 hours without any indication of wave activity (small-scale wave activity can sometimes be seen in the lidar data in form of a wavy structure in the time-altitude evolution of a cloud on typical timescales of 10–30 min, in the cases discussed here, this does not occur). Small-scale temperature and humidity fluctuations are therefore not a likely explanation for this observation.

[55] Nonvolatile material such as mineral dust is also not likely to be a component of these clouds. There is no reason why such a material should accumulate right at the cold point tropopause, while no depolarizing aerosol exists elsewhere in the TTL.

[56] *Luo et al.* [2003] proposed a stabilization mechanism for ultra thin tropical cirrus (UTTC) that were observed during the APE-THESEO campaign near the Seychelles in the western Indian Ocean [*Stefanutti et al.*, 2004]. While some thin clouds observed at Paramaribo can be explained by this mechanism (e.g., the layer at 16.2 km in Figure 5d), others cannot. The ETTCi detected on 16 November (Figure 6) lacks some of the prerequisites necessary for UTTC stabilization: the air at the cloud altitude is not saturated, nor is there evidence of supersaturation above. The clouds do not occur below the cold point, they rather occur slightly above as can be seen in Figure 6i (the radiosonde passed the CPT about 20 min after the last observation of the layer at 0705 UT, low clouds obscured the ETTCi afterward. Given the stability of the layer during the preceding hour, this time delay should not have an influence on the overall picture). Therefore it is unlikely that the observed layer is an ice cloud stabilized by a balance between steady updraft and sedimentation.

[57] We can only speculate on the nature of this layer, but the most plausible explanation we may provide is, that these layers are remnants of ice clouds which are stabilized by some inorganic acids like HNO_3. This hypothesis is supported by the fact that the CPT temperature is falling below the existence temperature of nitric acid trihydrate (NAT) [*Hanson and Mauersberger*, 1988] at the given partial pressures of H_2O and HNO_3. There has been considerable debate on the existence of NAT at the tropical tropopause. Some in situ measurements of cloud particles provided no evidence for an important role of HNO_3 in tropical cirrus clouds [*Peter et al.*, 2003]. On the other hand, *Hervig and McHugh* [2002] and *Popp et al.* [2006] claimed evidence for the presence of NAT in the tropics based on satellite and in situ observations, respectively. *Jensen and Drdla* [2002] argued that despite the low nitric acid concentration of 0.1–0.5 ppb, NAT particles could exist at the low temperatures of the tropical tropopause region and calculated a potential mass concentration of 0.2 $\mu g/m^3$. This is on the same order of magnitude as the concentration derived from the lidar observations for the extremely thin layers found on 11 and 16 November 2004 which was 0.4 $\mu g/m^3$ (Table 1). Given the large uncertainties in this retrieval, NAT could play an important role in explaining our observations.

[58] These layers are certainly irrelevant in terms of radiative transfer and most likely do not directly contribute to the dehydration of the air. The amount of water present in such particles (around 4 ppb) is far too low. However, these clouds could have an important influence on the transport of other trace gases into the stratosphere. They may also serve as nuclei for heterogeneous ice formation in case the relative humidity exceeds 100% by adiabatic cooling. In this case they could significantly lower the supersaturation necessary for cirrus formation and as a consequence they would indirectly enhance the dehydration of air entering the stratosphere.

5. Summary and Conclusions

[59] During the STAR pilot study in Paramaribo, Suriname (5.8°N, 55.2°W) a high-performance Raman lidar was successfully deployed at a tropical site. Measurements were made mainly during night time with the lidar, from 28 September to 16 November 2004. Daily radiosonde launches supplied temperature profiles and occasionally water vapor profiles were measured using a balloon-borne frost-point hygrometer. We report on this unique set of data that allows a detailed insight into the tropical tropopause region. We study clouds and the dehydration of air entering the stratosphere on the basis of the lidar and radiosonde data by using a trajectory model.

[60] The temporal coverage of cirrus was extremely large with 88%. There were very few occasions when persistently no clouds were present in the upper tropical troposphere. We show that the lidar ratio of tropical cirrus is with a mean value of 26 sr significantly higher compared to midlatitude cirrus (16 sr). This implies that the microphysical properties of tropical cirrus are different from midlatitude cirrus.

[61] The upper troposphere in the tropics is split into two regions by an upper tropospheric inversion (UTI) that regularly occurs about 2 km below the cold point tropopause. Subvisual cirrus most often occur in the TTL above the UTI. The coverage with subvisual cirrus in the tropics is clearly enhanced compared to the midlatitudes, suggesting that the lifetime of this type of cloud is extended by persistent large-scale ascent. Extremely thin cirrus clouds with optical depth below 10^{-3} occur frequently at the tropical cold point tropopause.

[62] The origin and the existence criteria of the cirrus clouds were investigated by observations and a newly developed trajectory model which calculates the vertical transport from diabatic heating rates. The results of three case studies discussed in detail suggest the following scenario for the formation and evolution of TTL cirrus: deep convection feeds moist air into the TTL. Inside the TTL the air is heated by long-wave radiation. It is subject to

steady slow ascent and adiabatic cooling. Visible cirrus clouds (optical depth about 0.1) which hold a significant amount of total precipitable water exist in this environment on a timescale of days and can therefore efficiently dehydrate the air. Episodic warming will cause the clouds to evaporate but subsequent cooling leads again to cloud formation, if another absolute temperature minimum and thus saturation is reached. The clouds at this stage are generally subvisual. These thin clouds hold only a few percent of the total water. However, since the updraft velocities are very small (on the order of 1 mm/s) and the life time of such clouds appears to be long, they may again cause some further dehydration of the air.

[63] The occurrence of dehydration is supported by our observation that air that, according to the trajectory model, had passed through a cold trap before it arrived at Paramaribo, in general, does not contain ice. The humidities measured by the Snow White sonde in previously dried (and hence cloud free TTL air) supports the hypothesis of dehydration to the minimum saturation vapor pressure along a trajectory.

[64] The hypothesis that clouds exist where saturation is reached along a trajectory and no clouds exist where air was efficiently dried in a cold trap and was subsequently warmed, explains a large fraction (70%) of the lidar observations of TTL cirrus. This result is only achieved when using diabatic heating rates instead of vertical winds from operational ECMWF data to calculate trajectories in the TTL. This demonstrates that vertical transport above the UTI is accomplished primarily by radiative heating and that cloud formation always occurs in saturated air. Since the lidar can measure only during clear sky conditions ($OD < 1$) we generally sampled TTL air masses only in a larger distance from deep convective zones. Nearby thunderstorms create cirrus up to about 14 km, but we did not find any evidence of an influence of such events at higher altitudes. However, the lofting of clouds by radiative heating as described by *Corti et al.* [2006] is a likely mechanism of feeding moist air from the outflow of deep convection into the TTL. The general pathway for troposphere-to-stratosphere exchange suggested by *Corti et al.* [2006] is consistent with our observations.

[65] The cloud coverage given in the operational ECMWF analysis matches well with the observation in the TTL. This was already explored by *Fortuin et al.* [2007] using the entire data set from the STAR pilot study in Paramaribo. It seems that the cloud parameterization used in the ECMWF [*Tiedtke*, 1993] simulates the cirrus formation in the TTL fairly well, while it has greater problems capturing cloud events in the upper troposphere when convective processes are dominating.

[66] *Fueglistaler et al.* [2005] showed that the humidity of the lower tropical stratosphere is reproduced by a model that assumes that air passing through the tropical tropopause is freeze dried to the saturation vapor pressure at the lowest temperature of its trajectory. This concept is supported by our observations. However, there are a number of open questions on the exact nature of the dehydration process: Theoretically, the formation of ice particles requires high supersaturation with RH_I around 160% [*Koop et al.*, 2000]. Moreover, it is unlikely that subvisual cirrus at the CPT are capable of dehydrating the air completely, i.e., to a RH_I of 100%. Indeed, there is evidence that the transport of water to the stratosphere involves a substantial contribution from evaporated water ice [*Keith*, 2000] suggesting that ice particles are transported into the stratosphere. As a consequence, air passing through the tropopause should on average have a higher humidity than given by the minimum ice saturation.

[67] In order to explain the dryness of the stratosphere these effects need to be balanced by other processes that increase dehydration. Heterogeneous ice nuclei and wave driven temperature fluctuation could play an important role in that respect [*Kärcher*, 2004]. However, other trace gases could also be of some importance. We found evidence for the existence of particles near the cold point tropopause in subsaturated air. Our observations are consistent with the presence of nitric acid trihydrate (NAT). These findings suggest that trace gases like HNO_3 could interfere in the process of cloud formation and dehydration at the tropical tropopause. If this is the case, the transport of water vapor into the stratosphere is controlled by a complex balance of dynamical, microphysical, and chemical effects that happen to yield in sum a stratospheric humidity close to the saturation vapor pressure of ice at the Lagrangian mean temperature minimum.

[68] **Acknowledgments.** We would like to thank Cor Becker and the staff at the MDS site in Paramaribo for their excellent support. Special thanks to Ingo Beninga, Tom Weinzierl and David Kaiser for performing some of the lidar measurements. The Snow White measurements were (partly) financed by the Netherlands Agency for Aerospace Program (NIVR). The ground equipment and the software for the Snow White sounding were provided by the project "Soundings of Ozone and Water in the Equatorial Region" (SOWER) and Holger Vömel, respectively. We like to thank the British Atmospheric Data Centre for performing trajectory calculations and the ECMWF for giving access to its database. This study was supported by the European Union's 6th framework program within the STAR (contract GOCE-CT-2003-506651) and O3-SCOUT (GOCE-CT-2004-505390) projects. Further financial support is acknowledged within the framework of the virtual institutes of the Helmholtz Associations "Pole-Equator-Pole" (PEP) and "Center for the tropical tropopause region" (ZTT).

References

Ansmann, A., U. Wandinger, M. Riesbel, C. Weitkamp, and W. Michaelis (1992), Independent measurement of extinction and backscatter profiles in cirrus clouds by using a combined Raman elastic-backscatter lidar, *Appl. Opt.*, *31*(33), 7113–7131.

Behrendt, A., and T. Nakamura (2002), Calculation of the calibration constant of polarization lidar and its dependency on atmospheric temperature, *Opt. Express*, *10*(16), 805–817.

Bonazzola, M., and P. H. Haynes (2004), A trajectory-based study of the tropical tropopause region, *J. Geophys. Res.*, *109*, D20112, doi:10.1029/2003JD004356.

Corti, T., B. P. Luo, Q. Fu, H. Vömel, and T. Peter (2006), The impact of cirrus clouds on tropical troposphere-to-stratosphere transport, *Atmos. Chem. Phys.*, *6*, 2539–2547.

Delval, C., B. Fluckiger, and M. J. Rossi (2003), The rate of water vapor evaporation from ice substrates in the presence of HCl and HBr: Implications for the lifetime of atmospheric ice particles, *Atmos. Chem. Phys.*, *3*, 1131–1145.

Folkins, I., M. Loewenstein, J. Podolske, S. Oltmans, and M. Proffitt (1999), A barrier to vertical mixing at 14 km in the tropics: Evidence from ozonesondes and aircraft measurements, *J. Geophys. Res.*, *104*(18), 22,095–22,102.

Fortuin, J., C. Becker, M. Fujiwara, F. Immler, H. Kelder, M. Scheele, O. Schrems, and G. Verver (2007), Origin and transport of tropical cirrus clouds observed over Paramaribo station, Surinam (6°N 55°W), *J. Geophys. Res.*, doi:10.1029/2005JD006420, in press.

Fueglistaler, S., M. Bonazzola, P. H. Haynes, and T. Peter (2005), Stratospheric water vapor predicted from the Lagrangian temperature history of air entering the stratosphere in the tropics, *J. Geophys. Res.*, *110*, D08107, doi:10.1029/2004JD005516.

Fujiwara, M., S.-P. Xie, M. Shiotani, H. Hashizume, F. Hasebe, H. Vömel, S. J. Oltmans, and T. Watanabe (2003a), Upper-tropospheric inversion and easterly jet in the tropics, *J. Geophys. Res.*, *108*(D24), 4796, doi:10.1029/2003JD003928.

Fujiwara, M., M. Shiotani, F. Hasebe, H. Vömel, S. Oltmans, P. Ruppert, T. Horinouchi, and T. Tsuda (2003b), Performance of the Meteolabor 'Snow White' chilled-mirror hygrometer in the tropical troposphere: Comparisons with the Vaisala RS80 A/H-Humicap sensors, *J. Atmos. Oceanic Technol.*, *20*(11), 1534–1542.

Gettelman, A., and P. M. de F. Forster (2002), A climatology of the tropical tropopause layer, *J. Meteorol. Soc. Jpn.*, *80*(4B), 911–924.

Gettelman, A., P. M. de F. Forster, M. Fujiwara, Q. Fu, H. Vömel, L. K. Gohar, C. Johanson, and M. Ammerman (2004), Radiation balance of the tropical tropopause layer, *J. Geophys. Res.*, *109*, D07103, doi:10.1029/2003JD004190.

Hanson, D., and K. Mauersberger (1988), Laboratory studies of the nitric acid trihydrate—Implications for the south polar stratosphere, *Geophys. Res. Lett.*, *15*, 855–858.

Hervig, M., and M. McHugh (2002), Tropical nitric acid clouds, *Geophys. Res. Lett.*, *29*(7), 1125, doi:10.1029/2001GL014271.

Heymsfield, A. (2003), Properties of tropical and midlatitude ice cloud particle ensembles. Part I: Median mass diameters and terminal velocities, *J. Atmos. Sci.*, *60*(21), 2573–2591.

Heymsfield, A. J., L. M. Miloshevich, C. Twohy, G. Sachse, and S. Oltmans (1998), Upper tropospheric relative humidity observations and implications for cirrus ice nucleation, *Geophys. Res. Lett.*, *25*(9), 1343–1346.

Immler, F., and O. Schrems (2002), Determination of tropical cirrus properties by simultaneous LIDAR and radiosonde measurements, *Geophys. Res. Lett.*, *29*(23), 2090, doi:10.1029/2002GL015076.

Jensen, E., and K. Drdla (2002), Nitric acid concentrations near the tropical tropopause: Implications for the properties of tropical nitric acid trihydrate clouds, *Geophys. Res. Lett.*, *29*(20), 2001, doi:10.1029/2002GL015190.

Jensen, E. J., et al. (2005), Ice supersaturations exceeding 100% at the cold tropical tropopause: Implications for cirrus formation and dehydration, *Atmos. Chem. Phys.*, *5*, 851–862.

Kärcher, B. (2004), Cirrus clouds in the tropical tropopause layer: Role of heterogeneous ice nuclei, *Geophys. Res. Lett.*, *31*, L12101, doi:10.1029/2004GL019774.

Keith, D. (2000), Stratosphere-troposphere exchange: Inferences from the isotopic composition of water vapor, *J. Geophys. Res.*, *105*(D12), 15,167–15,174.

Koop, T., B. Luo, A. Tsias, and T. Peter (2000), Water activity as the determinant for homogeneous ice nucleation in aqueous solutions, *Nature*, *406*, 611–614, doi:10.1038/35020537.

Luo, B., et al. (2003), Dehydration potential of ultrathin clouds at the tropical tropopause, *Geophys. Res. Lett.*, *30*(11), 1557, doi:10.1029/2002GL016737.

Manney, G., D. Allen, K. Krüger, J. Sabutis, S. Pawson, R. Swinbank, C. Randall, A. Simmons, and C. Long (2005), Diagnostic comparison of meteorological analyses during the 2002 Antarctic winter, *Mon. Weather Rev.*, *133*, 1261–1278.

McFarquhar, G., A. Heymsfield, J. Spinhirne, and B. Hart (2000), Thin and subvisual tropopause tropical cirrus: Observations and radiative impact, *J. Atmos. Sci.*, *57*(12), 1841–1853.

Meijer, E. W., B. Bregman, A. Segers, and P. F. J. van Velthoven (2004), The influence of data assimilation on the age of air calculated with a global chemistry-transport model using ECMWF wind fields, *Geophys. Res. Lett.*, *31*, L23114, doi:10.1029/2004GL021158.

Mishchenko, M. I., and K. Sassen (1998), Depolarization of lidar returns by small ice crystals: An application to contrails, *Geophys. Res. Lett.*, *25*(3), 309–312.

Morcrette, J.-J., S. Clough, E. Mlawer, and M. Iacono (1998), Impact of a validated radiative transfer scheme, RRTM, on the ECMWF model climate and 10-day forecasts, *Tech. Memo. 252*, 47 pp., Eur. Cent. for Med.-Range Weather Forecasts, Reading, U. K.

Oltmans, S. J., and D. J. Hofmann (1995), Increase in lower-stratospheric water vapour at a mid-latitude Northern Hemisphere site from 1981 to 1994, *Nature*, *374*, 146–149.

Peter, T., et al. (2003), Ultrathin Tropical Tropopause Clouds (UTTCs): I. Cloud morphology and occurrence, *Atmos. Chem. Phys.*, *3*, 1083–1091.

Popp, P. J., et al. (2006), The observation of nitric acid-containing particles in the tropical lower stratosphere, *Atmos. Chem. Phys.*, *6*, 601–611.

Randel, W., F. Wu, S. J. Oltmans, K. Rosenlof, and G. Nedoluha (2004), Interannual changes of stratospheric water vapor and correlations with tropical tropopause temperatures, *J. Atmos. Sci.*, *61*(17), 2133–2148.

Rosenlof, K. H., et al. (2001), Stratospheric water vapor increases over the past half-century, *Geophys. Res. Lett.*, *28*(7), 1195–1198.

Schäfer, H.-J., O. Schrems, G. Beyerle, B. Hofer, W. Mildner, and F. Theopold (1997), Shipborne measurements with a modular multipurpose mobile lidar system for tropospheric and stratospheric aerosol observations, *Proc. SPIE Int. Soc. Opt. Eng.*, *3104*, 265–273.

Scheele, M. P., P. C. Siegmund, and P. F. J. van Velthoven (2005), Stratospheric age of air computed with trajectories based on various 3D-Var and 4D-Var data sets, *Atmos. Chem. Phys.*, *5*, 1–7.

Seidel, D. J., R. J. Ross, J. K. Angell, and G. C. Reid (2001), Climatological characteristics of the tropical tropopause as revealed by radiosondes, *J. Geophys. Res.*, *106*(D8), 7857–7878.

Sonntag, D. (1994), Advances in the field of hygrometry, *Meteorol. Z.*, *3*, 51–66.

Spichtinger, P., K. Gierens, U. Leiterer, and H. Dier (2003a), Ice supersaturation in the tropopause region over Lindenberg, Germany, *Meteorol. Z.*, *12*(3), 143–156.

Spichtinger, P., K. Gierens, and W. Read (2003b), The global distribution of ice-supersaturated regions as seen by the Microwave Limb Sounder, *Q. J. R. Meteorol. Soc.*, *29*, 3391–3410, doi:10.1256/qj.02.141.

Stefanutti, L., et al. (2004), The APE-THESEO tropical campaign: An overview, *J. Atmos. Chem.*, *48*(1), 1–33.

Tegtmeier, S. (2006), Variationen der stratosphärischen Residualzirkulation und ihr Einfluss auf die Ozonverteilung, 179 pp., Ph.D. thesis, Math.-Naturwiss. Fak., Univ. Potsdam, Potsdam, Germany.

Thomas, A., et al. (2002), In situ measurements of background aerosol and subvisible cirrus in the tropical tropopause region, *J. Geophys. Res.*, *107*(D24), 4763, doi:10.1029/2001JD001385.

Tiedtke, M. (1993), Representation of clouds in large-scale models, *Mon. Weather Rev.*, *121*, 3040–3061.

Verver, G., M. Fujiwara, P. Dolmans, C. Becker, P. Fortuin, and L. Miloshevich (2006), Performance of the Vaisala RS80A/H and RS90 Humicap Sensors and the Meteolabor "Snow White" Chilled-Mirror Hygrometer in Paramaribo, Suriname, *J. Atmos. Oceanic Technol.*, *23*(11), 1506–1518, doi:10.1175/JTECH1941.1.

Vömel, H., M. Fujiwara, M. Shiotani, F. Hasebe, S. J. Oltmans, and J. Barnes (2003), The behavior of the Snow White chilled-mirror hygrometer in extremely dry conditions, *J. Atmos. Oceanic Technol.*, *20*, 1560–1567.

Wang, P.-H., P. Minnis, M. McCormick, G. Kent, and K. Skeens (1996), A 6-year climatology of cloud occurence frequency from Stratospheric Aerosol and Gas Experiment II observations (1985–1990), *J. Geophys. Res.*, *101*(D23), 29,407–29,429.

Whiteman, D. N., B. Demoz, and Z. Wang (2004), Subtropical cirrus cloud extinction to backscatter ratios measured by Raman Lidar during CAMEX-3, *Geophys. Res. Lett.*, *31*, L12105, doi:10.1029/2004GL020003.

Winker, D., and C. Trepte (1998), Laminar cirrus observed near the tropical tropopause by LITE, *Geophys. Res. Lett.*, *25*(17), 3351–3354.

P. Fortuin and G. Verver, Royal Netherlands Meteorological Institute, NL-3730 AE, De Bilt, Netherlands.

M. Fujiwara, Faculty of Environmental Earth Science, Hokkaido University, Sapporo 060-0810, Japan.

F. Immler and O. Schrems, Alfred-Wegener-Insitut für Polar- und Meeresforschung, Am Handelshafen 12, D-27570 Bremerhaven, Germany. (franz.immler@awi.de)

K. Krüger, Leibniz Institute of Marine Sciences at the University of Kiel (IFM-GEOMAR), Duesternbrooker Weg 20, D-24105 Kiel, Germany.

S. Tegtmeier, Department of Physics, University of Toronto, Toronto, ON, Canada M5S 1A7.